IEEE Access
Multidisciplinary | Rapid Review | Open Access Journal

Received 29 July 2022, accepted 15 September 2022, date of publication 21 September 2022, date of current version 30 September 2022.

Digital Object Identifier 10.1109/ACCESS.2022.3208352

RESEARCH ARTICLE

A Sensitive and Accurate Walking Speed Prediction Method Using Ankle Torque Estimation for a User-Driven Treadmill Interface

SANGHUN PYO, HOSU LEE, AND JUNGWON YOON, (Member, IEEE)
Institute of Integrated Technology, Gwangju 61005, South Korea
Gwangju Institute of Science and Technology (GIST), Gwangju 61005, South Korea

Corresponding author: Jungwon Yoon (jyoon@gist.ac.kr)

This work was supported in part by the "Practical Research and Development Support Program supervised by the GTI—Gwangju Institute of Science and Technology (GIST) Technology Institute" funded by GIST, in 2022; and in part by the National Research Foundation (NRF) of Korea under Grant 2019M3C1B8090798.

This work involved human subjects or animals in its research. Approval of all ethical and experimental procedures and protocols was granted by the Institutional Review Board of Gwangju Institute of Science and Technology under Approval No. 20210217-HR-59-06-04, and performed in line with the Declaration of Helsinki.

ABSTRACT To achieve safe and immersive interface with a user-driven treadmill (UDT), robustness of the user position must be ensured by sensitively estimating and accurately converging to the intentional walking speed (IWS). The existing IWS estimation using a linear observer with the cart model (1st order dynamics) can exponentially converge to the true IWS. However, when the estimation sensitivity is increased by increasing the gain, this method causes severe postural instability due to the generation of excessive anomalous forces. Thus, the existing method has an implicit limitation with regards to increasing the position robustness because of the postural instability issues. In this paper, to simultaneously achieve sensitive and accurate IWS estimation while reducing postural instability on a UDT, in addition to the cart model, we have also utilized the inverted pendulum-based gait model (IPGM) as a 2nd order dynamic to estimate the intentional walking acceleration (IWA) generated by the ankle torque. Thus, the proposed IWS prediction method uses the cart model for accurate convergence to IWS and the IPGM to follow sensitively the change in the IWS. In the proposed method, the internal states of the existing observers applied to the 1st and 2nd order dynamics are shared recursively to estimate the ankle torque acting as a disturbance for the IPGM and to sensitively predict the change in the IWS. Experiments show that the proposed method can significantly facilitate the users in following a profile of desired walking speeds more accurately than the existing IWS estimation method under the same position robustness setup.

INDEX TERMS Gait dynamics, locomotion interface, user-driven treadmill, disturbance observer.

I. INTRODUCTION

Treadmills are widely utilized in virtual reality (VR) as a representative device for locomotion interface (LI) to allow users to participate actively in VR with realistic spatial sensations [1], [2], [3]. This functionality is achieved through a user-driven treadmill (UDT) that tracks the user's locomotion intention and allows the generation of unlimited level-ground conditions without limiting the user's motions. To ensure safe and immersive gait interface with a UDT, the user's position must be maintained in a reference position above the treadmill belt even when their walking speed is changing arbitrarily, and their spatial and temporal gait parameters should not be significantly different from those during over-ground or conventional treadmill walking [4], [5].

If the belt motion of a UDT does not sensitively follow a user's intentional walking speed (IWS), it causes a position error, the excess of which can induce the user to fall down. Thus, the main objectives of a UDT control scheme are to ensure the position robustness by accurately estimating the IWS, and to generate the appropriate control commands when the user dynamically changes their walking speed [5], [6].

The associate editor coordinating the review of this manuscript and approving it for publication was Mark Kok Yew Ng.

A general method of configuring the UDT controller consists of a feed-forward term for estimating the IWS and a feedback term to compensate for the user's position error [7], [8]. Position robustness is affected by both these terms; however, the feed-forward term is mainly related to postural stability [5], [6].

The user's IWS is considered as a disturbance input for the UDT because their walking behavior causes their position to change. Thus, the IWS can be estimated from the position information of the user's center of mass (COM) [9], [10], [11], [12]. Souman *et. al.* proposed an IWS estimation scheme using a stable linear observer that converges precisely to the steady state value of the IWS [12]. This is the representative UDT controller that can perform LI by using only the position of the user's COM. To design the linear observer that works as the feedforward component in the research reported in [12], the authors used a simple cart model as the 1st order dynamics (velocity-level control), which can exponentially and precisely converge to the true IWS.

However, Kim. *et. al.* [13] reported that, when using a large gain for the linear observer to increase the position robustness by sensitively converging to the IWS, a generated anomalous force affects the user's postural stability and increases the risk of falling. Since the existing IWS estimator uses the 1st order dynamics (cart model) that differ greatly from the human walking dynamics, such as the lack of consideration for lower limb movement, it cannot appropriately estimate the acceleration or deceleration occurring in the changing IWS on a UDT. On the contrary, the observer with a low gain setting cannot guarantee the position robustness with respect to a reference position due to a relatively long time constant. Therefore, there is a limited margin to simultaneously improve the overall performance in terms of position robustness and postural stability.

Among other IWS estimation methods, Yoon. *et. al.* proposed a method that involves the maximum swing-foot velocity (MSFV) as a consideration of the bipedal motion of human gait [5]. According to the kinematic model of the normal gait pattern, the MSFV has a linearly proportional relationship with the average gait speed during a single footstep. By using the MSFV instead of the position of the COM, this method can significantly alleviate the postural instability issue even though it sensitively estimates the IWS, unlike the method reported in [12]. However, this estimation method discretely updates the IWS because it needs time to determine the MSFV from the swing-foot velocity during one step. Moreover, since it is based on the kinematic model of a normal gait pattern, it suffers from inaccurate prediction of the IWS when the user is starting to walk from a standstill (i.e., from zero to preferred speed). Thus, it is difficult to apply it to a wide range of walking patterns and speeds.

To alleviate the limitations of the works presented in [5] and [12], Kim. *et. al.* proposed a feedforward strategy called the attenuator [13], which can keep a time required to converge to the IWS by attenuating from an exponential convergence rate (linear observer) to a proportional rate based on the MSFV method. However, while using the attenuator concept, it may still be difficult to guarantee the position robustness due to the reduced convergence rate when the gait speed is changing dynamically.

Therefore, in the presented work, we have aimed to design a walking speed prediction method that can sensitively respond to changes in the IWS to increase position robustness, while overcoming the postural instability by using an appropriate gait dynamics model. The proposed method involves simultaneous utilization of the existing 1st order dynamics to guarantee the accurate IWS convergence and the 2nd order dynamics of the inverted pendulum-based gait model (IPGM) [14], [15] to represent the movement of the lower extremities. While the conventional method involving the 1st order dynamics tracks the true IWS, another disturbance observer working with the 2nd order dynamics detects the amount of change in the IWS through the estimation of the ankle torque.

The effectiveness of the proposed method is validated through experimentation with 10 subjects where it is compared to the existing controller reported in [12]. The experiment results revealed that use of the proposed method allowed the subjects to change their gait speed more accurately according to cue speeds given to them as reference commands, while maintaining the position robustness at the same level as the conventional method.

II. DESIGN OF WALKING SPEED PREDICTION METHOD

A. GAIT DYNAMICS CONSIDERING ANKLE TORQUE

The existing IWS estimation, which is based on the cart model shown in Figure 1 [12], has the problem of gait instability that occurs when a user tries to change their walking speed [13]. According to the research reported in [12], the true IWS (v_w) acting as a disturbance in a UDT can be estimated using the cart model, and it can be expressed as follows

$$\dot{x}_1 = -v_c + v_w = -v + v_w \tag{1}$$

where, x_1 is the position of the COM, v_w denotes the true IWS, which is considered as the disturbance of Eq. (1), and v_c and v are the control command and the current UDT velocity, respectively. For simplicity, both these values are the same since it is assumed that the low-level controller utilized in the UDT can precisely follow the control command, and x_1 can be represented as the position error when the desired position (x_{ref}) is considered to be zero (i.e., $x_{ref} = 0$).

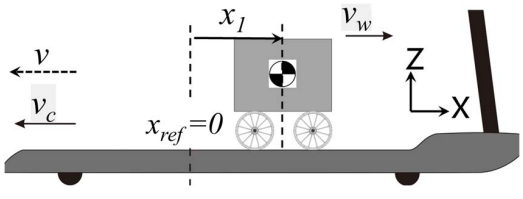

FIGURE 1. Simplified UDT dynamics based on the cart model (1st order dynamics) represented by Eq. (1).

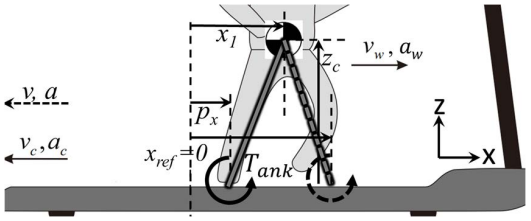

FIGURE 2. Expanded UDT dynamics according to the inverted pendulum model-based gait model (2nd order dynamics) represented by Eq. (2).

When the UDT tries to follow the IWS based on the position error (x_1), it is difficult to sensitively estimate the IWS because it may implicitly include a delay. Therefore, additional information that can be used to quickly estimate the change in IWS is required. To design the IWS estimator based on the human gait dynamics [14], the cart model given in Eq. (1) is differentiated to extend it to 2nd order dynamics, as follows

$$\begin{cases} \dot{x}_1 = x_2 \\ \dot{x}_2 = -a_c + a_w = -a + a_w \end{cases} \tag{2}$$

where x_1 and x_2 represent the position and velocity of the COM, respectively, a_w denotes the intentional walking acceleration (IWA) generated by the ankle torque, which is considered as the disturbance in Eq. (2), and a_c is the final control command for UDT belt acceleration (a). To consider the human gait motion, the IWA represented as a_w can be rewritten by applying the IPGM [15], as follows:

$$a_w = \dot{v}_w = \frac{gx_1}{z_c} - \frac{gp_x}{z_c} + \frac{T_{ank}}{mz_c} \tag{3}$$

where g is the gravitational acceleration defined as $9.81 m/s^2$, m is the user's mass, T_{ank} represents the generated ankle torque, and z_c and p_x are the height of the user's COM and their ankle joint position during the stance phase, respectively. Since the relative position of the ankle joint (p_x) and the COM (x_1) can be easily measured using an optical sensor system, the unknown input (disturbance) of Eq. (3) is the ankle torque (T_{ank}) related to IWA and IWS.

As shown in Figure 2, the IPGM considers the torque generated at the ankle joint while performing the ground-pushing motion. Thus, if the generated ankle torque (T_{ank}) can be estimated using the user's kinematic information (p_x, x_1) and the current speed and acceleration of the treadmill belt (v_c, a_c), a more accurate IWS estimation can be achieved.

B. THE PROPOSED LI CONTROLLER

In the proposed IWS prediction method, which applies the additional disturbance observer based on the IPGM is shown in Figure 3. The proposed method utilizes the sum of the two observed values to achieve accurate convergence to the IWS ($\hat{v}_w$) and fast response to the change in IWS ($\hat{x}_2$). Similar to the strategies used in previous LI research [5], [9], [12], [13], the proposed LI controller utilizes the robust integration of the sign of the error (RISE) controller [16] for the feedback

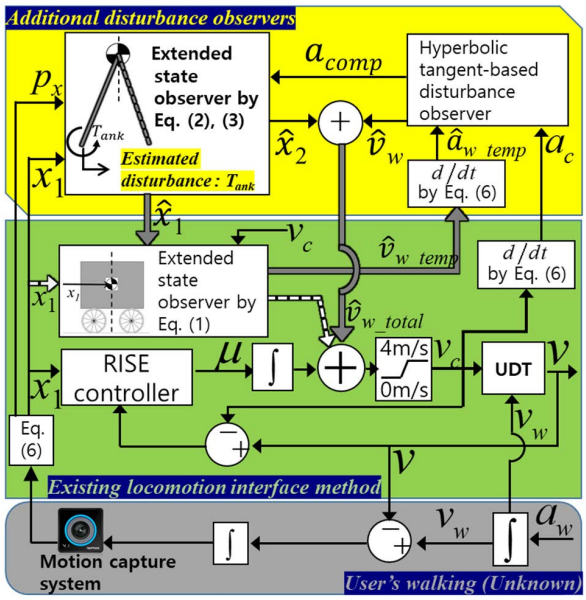

FIGURE 3. The proposed LI controller with the additional disturbance observer.

term (μ). This feedback control scheme helps to increase the robustness of the position error by estimating the slowly time-varying uncertainty of the closed-loop system.

In the existing LI method without the additional disturbance observer, the true IWS (v_w) is observed by the extended state observer (ESO) [18] based on the cart model only, as given by Eq. (1), and it directly feeds forward to the final control command (v_c), shown using the white-dashed line in Figure 3. Therefore, according to the existing method for designing a LI controller, the conventional control command can be given as follows

$$v_c(t) = \int_0^t \mu(\tau) d\tau + \hat{v}_{w\_temp} \tag{4}$$

where $\hat{v}_{w\_temp}$ is the value observed by the ESO based on Eq. (1) and μ is the feedback command from the RISE controller. The key feature of $\hat{v}_{w\_temp}$ is exponential convergence to v_w according to the property of the 1st order dynamics.

Meanwhile, to sensitively predict the change in the IWS by estimating the generated ankle torque (T_{ank}) in the IPGM, the additional disturbance observer is utilized as shown in Figure 3 (Gray-line), and the conventional control command represented by Eq. (4) is modified by utilizing the additional disturbance observer as follows:

$$v_c(t) = \int_0^t \mu(\tau) d\tau + \hat{v}_w + \hat{x}_2 = \int_0^t \mu(\tau) d\tau + \hat{v}_{w\_total} \tag{5}$$

where $\hat{x}_2$ is the observed amount of change in the IWS, which is computed by the 2nd order dynamics represented by Eq. (2) and (3), $\hat{v}_w$ is observed using the hyperbolic tangent tracking differentiator-based nonlinear disturbance observer (HTDO) [17] to accurately converge to the steady-state IWS with the disturbance rejection property, and $\hat{v}_{w\_total}$ is the summation of these observed values.

In Eq. (5), $\hat{x}_2$ can be detected during the swing phase, which allow the IWS estimation within a half-step period. This feature is similar to the concept proposed by Yoon *et. al.* [5]. Thus, the IWS estimation can be updated immediately, while the other foot (stance foot) generating the ankle torque is still on the UDT. This can also help prevent falling on the treadmill by quickly updating the UDT speed [18].

As shown in Figure 3, inputs of the HTDO are the acceleration-level values given as $\hat{a}_{w\_temp}$, and a_c, which are calculated by the tracking differentiator (TD) [19] utilized between the 1st order dynamics-based ESO and the HTDO to obtain better signal processing results of the differentiation than the finite difference methods. TD works well for practical engineering problems because it can extract the continuously filtered signal and its differential value from randomly noisy or discontinuous signal data [18]. In this paper, the nonlinear TD constructed using the hyperbolic tangent (HT) nonlinear function-based TD (HTTD) is utilized as follows: [20]

$$\begin{cases} \dot{z}_1 = z_2 \\ \dot{z}_2 = -\rho^2 \left[m_1 \tanh\left(z_1 - z_{input}\right) + m_2 \tanh\left(z_2/\rho\right) \right] \end{cases} \tag{6}$$

where, ρ, m_1 and m_2 are positive design parameters, z_{input} is the input value that requires signal processing, z_1 is the output value after signal processing, and z_2 is a state representing the differential value of z_1. Moreover, the HTTD is also applied to the motion capture system to reduce the random noise in the measured position of the COM (x_1) and the ankle joint position (p_x), as shown in Figure 3.

In this paper, to properly estimate the ankle torque (T_{ank}), the cart model with exponential convergence property is also used to estimate the IWS precisely and sensitively. By applying the additional disturbance observer to the existing method, the proposed method helps to increase position robustness while mitigating the postural instability.

C. DESIGN OF AN OBSERVER FOR ESTIMATING THE AMOUNT OF CHANGE IN IWS ($\hat{x}_2$)

In the IPGM shown in Figure 2, IWA (a_w) is generated by T_{ank} in Eq. (3). Thus, the ESO is utilized to estimate the ankle torque in real time as follows

$$\begin{cases} \dot{\hat{x}}_1 = -\beta_1 f\left(\varepsilon, \alpha_1, \xi\right) + \hat{x}_2, \quad \varepsilon = \hat{x}_1 - x_1 \\ \dot{\hat{x}}_2 = -\beta_2 f\left(\varepsilon, \alpha_2, \xi\right) + \dfrac{g\hat{x}_1}{z_c} - \dfrac{gp_x}{z_c} \\ \qquad\qquad + \left(\dfrac{\hat{x}_3}{z_c} + a_{comp}\right) - a_c \\ \dot{\hat{x}}_3 = -\beta_3 f\left(\varepsilon, \alpha_3, \xi\right) \simeq T_{ank}/m \end{cases} \tag{7}$$

where, β_1, β_2, β_3, α_1, α_2, α_3 and ξ are the gain parameters of the ESO. ε is an error value, which is computed based on the user position (x_1) and the state, $\hat{x}_1$, of the ESO. $\hat{x}_1$ is the observed value of the user position. $\hat{x}_2$, which is the value to be used as the control input, represents the amount of change in the IWS due to the estimated disturbance (ankle torque) represented as $\hat{x}_3$, a_{comp} is the estimated disturbance value predicted by the other observer to compensate for the uncertainties generated by the estimation error in $\hat{x}_3$.

In Eq. (7), f is a nonlinear gain function about ε, given as

$$f\left(\varepsilon, \alpha, \xi\right) = \begin{cases} \dfrac{\varepsilon}{\xi^{1-\alpha}}, & |\varepsilon| \le \xi \\ |\varepsilon|^{\alpha} \operatorname{sgn}\left(\varepsilon\right), & |\varepsilon| > \xi, \end{cases} \qquad 0 \le \alpha \le 1,\ \xi > 0 \tag{8}$$

If α is set to 1, this ESO becomes the Luenberger observer (Linear observer) because the output of the nonlinear gain function becomes identical to the input error (ε). On the other hand, it takes the form of a sliding mode observer when α is set to 0. Thus, if the value of α is increasing, the ESO is at a sensitive setting. Under $\alpha = 0$, the maximum value of f (ε, 0, ξ) defined by the sliding mode observer mode is just 1. When $0 < \alpha < 1$, the function f has the characteristic that the smaller the error, the relatively greater is the output and the larger the error, the smaller is the output.

To stably converge to the unknown input of the IPGM given by $\hat{x}_3$, the error dynamics ($\dot{\mathbf{E}}_{dy}$) is derived from Eq. (2), (3) and (7) as follows

$$\begin{aligned} \dot{\mathbf{E}}_{dy} &= \begin{bmatrix} -\beta_1 & 1 & 0 \\ \dfrac{g}{z_c} - \beta_2 & 0 & 1 \\ -\beta_3 & 0 & 0 \end{bmatrix} \begin{bmatrix} \hat{e}_1 \\ \hat{e}_2 \\ \hat{e}_3 \end{bmatrix} + \begin{bmatrix} 0 \\ 1 \\ 0 \end{bmatrix} \left(a_{comp} - a_c\right) \\ &= \mathbf{A}\vec{E} + \vec{B}\left(a_{comp} - a_c\right) \end{aligned} \tag{9}$$

where, $\hat{e}_1$, $\hat{e}_2$ and $\hat{e}_3$ are states of the error dynamics obtained by subtracting Eq. (2) and (3) from Eq. (7) (i.e., $\hat{e}_1 = \hat{x}_1 - x_1 = \varepsilon$, $\hat{e}_2 = \hat{x}_2 - x_2$, $\hat{e}_3 = \hat{x}_3 - x_3$). It should be noted that, since f is working as only a nonlinear gain with respect to ε, Eq. (9) is calculated by replacing $\hat{e}_1$ with f (ε, α, ξ) for the simplified stability analysis [21]. Thus, the solution of Eq. (9) is computed as

$$\mathbf{E}_{dy}\left(t\right) = e^{\mathbf{A}t}\mathbf{E}_d\left(0\right) + e^{\mathbf{A}t}\int_0^t e^{-\mathbf{A}\tau}\vec{B}\left(a_{comp} - a_c\right)d\tau \tag{10}$$

To find the bounded condition of Eq. (10) for any time (t), $\mathbf{A}$ in the error dynamics should be Hurwitz. Assuming that a_{comp} is bounded and z_c is closed, the gain satisfying the Hurwitz condition is given as

$$\beta_2 - \beta_3 > 9.81/z_c \tag{11}$$

To correspond to a height of the COM, which is different for each person, the gain should be set as $\beta_2 \gg \beta_3$.

For immersive LI, the gain should be set to match the generated ankle torque during real human walking by adjusting the gain parameters of the ESO ($\hat{x}_1 \rightarrow x_1(t)$ and $\hat{x}_3 \rightarrow T_{ank}/m$). In research on gait analysis [22][23], the maximum ankle torque (Nm) per body weight (kg) in the normal walking speed range (1.25~2 m/s) is known to be approximately 1.3 to 2 Nm/kg. Thus, the gains were set as; $\beta_1 = 10$, $\beta_2 = 360$, $\beta_3 = 290$, $\alpha_1 = 0.4$, $\alpha_2 = 0.4$, $\alpha_3 = 0.25$ and $\xi = 0.001$, so that $\hat{x}_3$ converges to the ankle joint torque trends suggested in the existing gait research. Moreover, the stability is also satisfied for the height of COM just above 0.14m

D. DESIGN OF AN OBSERVER FOR CONVERGING TO THE ACCURATE IWS ($\hat{v}_w$)

Through gain tuning, $\hat{x}_3$ was suggested to estimate the ankle torque, which causes the IWS change ($\hat{x}_2$). However, it is difficult to predict $\hat{x}_2$ accurately, since the estimated ankle torque ($\hat{x}_3$) is highly gain-dependent, and the available information is too limited to determine it correctly. Therefore, a_{comp}, mentioned in the previous section, needs to be applied to compensate for this inaccuracy.

Similar to the design method used for the observer reported in the previous research [12], which uses the cart model shown in Figure 1, the ESO based on the 1st order dynamics given by Eq. (1) is designed as follows

$$\begin{cases} \dot{\hat{x}}_a = -v_c - \hat{v}_{w\_temp} - \beta_{a1} f\left(\varepsilon_a, \alpha_{a1}, \xi_a\right) \\ \dot{\hat{v}}_{w\_temp} = -\beta_{a2} f\left(\varepsilon_a, \alpha_{a2}, \xi_a\right), \end{cases} \qquad \varepsilon_a = \hat{x}_a - \hat{x}_1 \tag{12}$$

where β_{a1}, β_{a2}, α_{a1}, α_{a2} and ξ_a are the positive control parameters, ε_a is the error in the observed values between $\hat{x}_1$ from the 2nd order dynamics-based ESO of Eq. (7) and its state, $\hat{x}_a$, of Eq. (12), and $\hat{v}_{w\_temp}$ represents the observed IWS based on the 1st order dynamics. To identify a user's intention quickly so that $\hat{v}_{w\_temp} \rightarrow v_w$, this ESO is sensitively setup with a high sensitivity for the observed user position obtained from Eq. (7).

For the stability analysis of this ESO, the characteristic equation, E_{dy_a}, of the error dynamics is computed as follows

$$E_{dy\_a}(s) = \frac{1}{s^2 + \beta_{a1} s + \beta_{a2}} \tag{13}$$

Thus, the 1st order dynamics-based ESO can be stable when all poles are in the left-half plane. Furthermore, to quickly converge to a user's steady state IWS, the conditions for exponential convergence to IWS are as follows

$$-\beta_{a1} \pm \sqrt{\beta_{a1}^2 - 4\beta_{a2}} < 0, \quad \beta_{a1}^2 > 4\beta_{a2} \tag{14}$$

Therefore, the gains of the ESO are set as; $\beta_{a1} = 40$, $\beta_{a2} = 300$, $\alpha_{a1} = 0.4$, $\alpha_{a2} = 0.4$ and $\xi_a = 0.001$. With the $\hat{v}_{w\_temp}$ from Eq. (12), a_{comp} in Eq. (7) is estimated by the HTDO as follows [19]

$$\begin{cases} \dot{\hat{v}}_w = -a_c + \left(\hat{a}_{w\_temp} + a_{comp}\right) \\ \dot{a}_{comp} = -\rho_z^2 \left[m_{z1} \tanh\left(\hat{v}_w - \hat{v}_{w\_temp}\right) + m_{z2} \tanh\left(a_{comp}/\rho_z\right) \right] \end{cases} \tag{15}$$

where, ρ_z, m_{z1} and m_{z2} are positive design parameters, $\hat{a}_{w\_temp}$ is computed using the $\hat{v}_{w\_temp}$ predicted by Eq. (12), and $\hat{v}_w$ is the accurate IWS compensated by a_{comp}, which is used as the control input for v_{w_total} in Eq. (5).

For the stability analysis of HTDO, it satisfies the convergence condition as follows [24]

$$\lim_{\rho_z \rightarrow \infty} \int_0^T \left| \hat{v}_w(t) - \hat{v}_{w\_temp}(t) \right| dt = 0 \; (any T > 0) \tag{16}$$

When $\rho_z \rightarrow \infty$, the stability analysis can be obtained as follows

$$\left|\dot{a}_{comp}\right| = \left| -\rho_z^2 \left[m_{z1} \tanh\left(\hat{v}_w - \hat{v}_{w\_temp}\right) + m_{z2} \tanh\left(a_{comp}/\rho_z\right) \right] \right| \tag{17}$$

Which means that the variation in a_{comp} is much faster than $-a_c + \hat{a}_w$. This can be clarified by the following equations.

$$\begin{cases} \lim\limits_{\rho_z \rightarrow \infty} \dfrac{d\left(-a_c + \left(\hat{a}_{w\_temp} + a_{comp}\right)\right)}{dt} = \dot{a}_{comp} \\ \lim\limits_{\rho_z \rightarrow \infty} \dfrac{-a_c + \left(\hat{a}_{w\_temp} + a_{comp}\right)}{\rho_z} = \dfrac{a_{comp}}{\rho_z} \end{cases} \tag{18}$$

Thus, when we regard "$-a_c + \left(\hat{a}_{w\_temp} + a_{comp}\right)$" as "$\hat{v}_w$", it is clear that Eq. (15) and Eq. (16) are established by the theorem reported in [25]. It should be noted that, in an actual system, $-a_c$ is bounded due to the physical limitations. Therefore, it is reasonable to assume that a_{comp} is estimated much faster than $\hat{a}_{w\_temp} - a_c$. Moreover, a_{comp} must be bounded because $\hat{a}_{w\_temp}$ is bounded by the 1st order dynamics-based ESO and the HTTD. Finally, the parameters of the HTDO are set as; $\rho_z = 10$, $m_{z1} = 1$ and $m_{z2} = 6$.

To briefly explain the proposed IWS prediction method shown in Figure 4, the HTDO calculates the compensated IWS ($\hat{v}_w$), and for an accurate IWA, it estimates the compensation value as a_{comp} which is the convergence error in the IWS calculated by the previous final control command (a_c) and the predicted IWA ($\hat{a}_{w\_temp}$) based on the 1st order dynamics. Next, the ESO based on the IPGM computes the amount of change in IWS ($\hat{x}_2$), and supplies $\hat{x}_1$ to the ESO based on the cart model with improved accuracy achieved by using a_{comp}. Again, in the cart model based ESO, the temporal IWS ($\hat{v}_{w\_temp}$) is re-estimated by the predicted user location update ($\hat{x}_1$), and the temporal predicted IWS ($\hat{v}_{w\_temp}$) is supplied to the HTDO to recursively improve the accuracy of IWS estimation. Thus, it helps to converge to more accurate IWS and T_{ank}/m values.

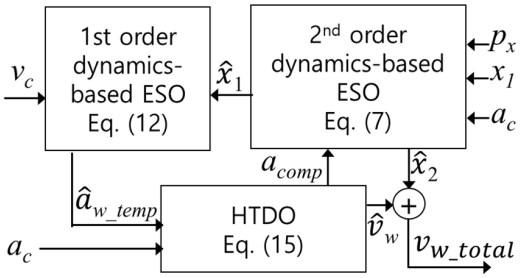

FIGURE 4. Flow chart to illustrate the relationship between each observer's input and output values.

E. FEEDBACK CONTROL

The primary objective of the feedback controller is to generate a control command to set the position of the user at a desired location. For this purpose, the feedback controller needs to be designed as shown in Figure 5 (See also Figure 3).

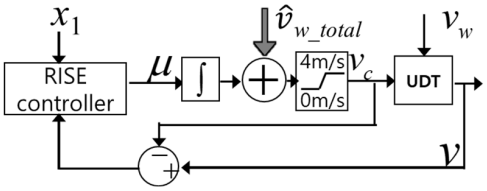

FIGURE 5. The feedback controller utilized in this work.

This controller utilizes the RISE controller given by [26]

$$\varepsilon_R = \dot{x}_1 + \alpha_1 x_1$$
$$\mu = (k_s + 1)(\varepsilon_R) + \int_0^t \left[\alpha_2 (k_s + 1)\varepsilon_R + \beta \mathrm{sgn}(\varepsilon_R)\right] \mathrm{d}\tau \tag{19}$$

where k_s, α_1, α_2 and β are adjustable positive control gains, and sgn$(\cdot)$ denotes the standard signum function. Now, when the error signal between the final control command (v_c) and the current belt speed (v) is defined as $q = v\text{-}v_c$, the final control command using Eq. (4) and (19) and the 1st order dynamics given in Eq. (1) is derived as follows [9]

$$v_c = \tilde{v}_w + k_a \int_0^t q(\tau)\,\mathrm{d}\tau + (k_s + 1)\alpha_2 \int_0^t \varepsilon_R\,\mathrm{d}\tau + \beta \int_0^t \mathrm{sgn}(\varepsilon_R)\,\mathrm{d}\tau, \tag{20}$$

where, k_a is an adjustable control gain. The controller defined in Eq. (20) renders the closed-loop dynamic as $\dot{q} = -kaq$ to compensate the error in the velocity command sent to the low-level controller (i.e., the servo system for actuating the treadmill belt), which demonstrates exponential convergence of q to zero. Thus, in this paper, it is assumed for simplicity that v_c and v are equal. The gain settings of the feedback controller are; $k_a = 1$, $k_s = 0.3$, $\alpha_1 = 0.01$, $\alpha_2 = 0.01$ and $\beta = 0.001$.

For safety purposes, the control command (v_c) is applied to the saturation block eliminating oscillation, which is set to $0\sim4m/s$. Thus, it does not generate the control command to move the user in the forward direction when they are positioned behind the reference location after they stop walking. The stability issue caused by the applied saturation is eliminated by a supervisory algorithm that initializes the integral term of the RISE controller when the user stays behind the reference position [9].

F. SIMULATION TO VERIFY THE PROPOSED METHOD

For intuitively understanding how the proposed IWS prediction method is working, a simulation was performed using the general walking speed and movement of the ankle joint. Since the proposed method uses the ankle joint position (p_x), it is necessary to simulate proper human gait kinematics. The research reported in [5] shows that the ankle joint positions of both the lower limbs can be considered as sinusoidal functions with opposite phases. When walking at a normal gait speed of about 1.4 m/s, the gait frequency and step length (magnitude of the sinusoidal function) can be modelled as

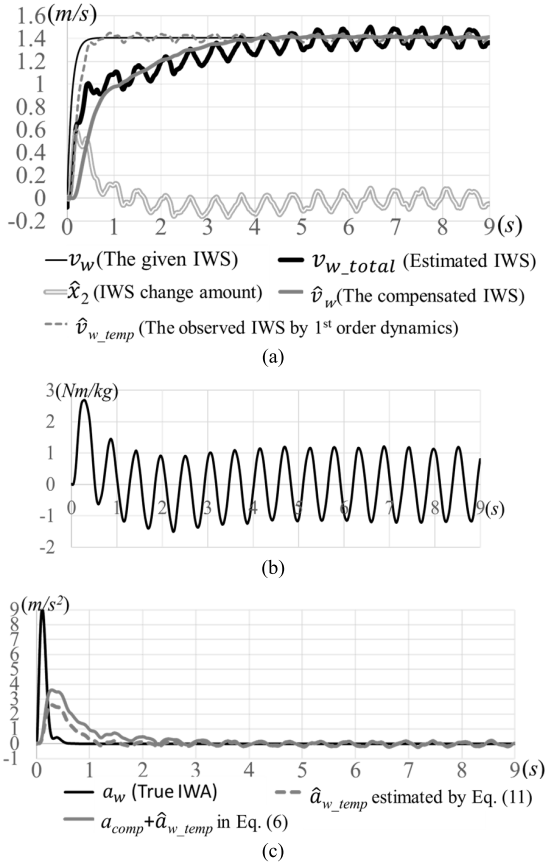

FIGURE 6. Simulation results, (a) Results for each observer, (b) Estimated ankle torque ($\hat{x}_3$), (c) IWA compensation by a_{comp} in the HTDO.

about 2Hz and 0.73 m [27], respectively. Thus, when the given IWS is set to $1.4m/s$, the ankle position, p_{both}, of both the lower limbs is updated as follows:

$$p_{both} = \begin{cases} x_1 + 0.73\sin(4\pi t) \\ x_1 + 0.73\sin\left(4\pi t + {}^1\!/_4\right) \end{cases} \tag{21}$$

where t is the simulation time. It should be noted that p_x is selected from p_{both} as the ankle joint position of the lower extremity that is in the stance phase. During the double support phase of gait, this is calculated as the average of the positions of the two ankle joints, and this value is almost equal to the position of the COM. To perform the simulation as close to the implemented system as possible, the random noise of the motion capture camera was included in the simulation in the range of ±1 mm. The loop frequency of the motion capture was set to 100Hz, and that of the controller was set to 1kHz.

In the simulation result shown in Figure 6(a), the given IWS (v_w) is $1.4m/s$ and the applied time constant is $0.1s$. The 1st order dynamics-based ESO converges quickly to the IWS but is affected by the oscillatory movement of the ankle position, while $\hat{v}_w$ stably converges to the steady state IWS with noise rejection.

Meanwhile, By using the estimated T_{ank}/m, as shown in Figure 6(b), $\hat{x}_2$ can sensitively respond to the amount

of change in the IWS and is reduced when the IWS goes to a steady state. In Figure 6(b), during the acceleration period, T_{ank}/m has a magnitude of 2.6 Nm/kg, approximately. Whereas, during the steady state of IWS, a magnitude of 1.3 Nm/kg is generated through the set gains. In human gait, a walking speed offset of approximately 0.25 m/s occurs at normal gait speed when a torque is generated at the ankle joint during the stance phase [5]. This trend is also observed in the proposed IWS estimator, as shown in Figure 6(a). Thus, the proposed scheme can interface with the users through control commands in a way that is closer to the real gait model than the observer based on the cart model only.

In Figure 6(c), $\hat{a}_{w\_temp}$, which is estimated by the 1st order dynamics-based ESO, has a relatively large difference from the true acceleration, given as a_w. However, due to the use of a_{comp}, this difference tends to be compensated compared to using only $\hat{a}_{w\_temp}$, and this compensated acceleration helps in achieving a fast response to $\hat{x}_2$ because Eq. (7) becomes more sensitive to the change in IWS.

III. METHOD

A. EXPERIMENTAL SETUP

Experiments were conducted to evaluate the performance of the proposed IWS prediction method compared to the existing controller. For conducting the experiment, we built the UDT system shown in Figure 7, the specifications of which are summarized in Table 1. The reduction ratio between the servomotor and the pulley attached to the drum driving the treadmill belt is 3.57. The utilized servo and PCI-type PLC are manufactured by YASKAWA, and their model names are SGM7G-20A and MP3100, respectively. The system can reach a maximum belt speed of 4.4 m/s when the servo is run at its rated maximum rotation speed of 3000 RPM. However, we limited the maximum rotation speed of the servo to 80% of the rated speed to maintain a performance margin. Thus,

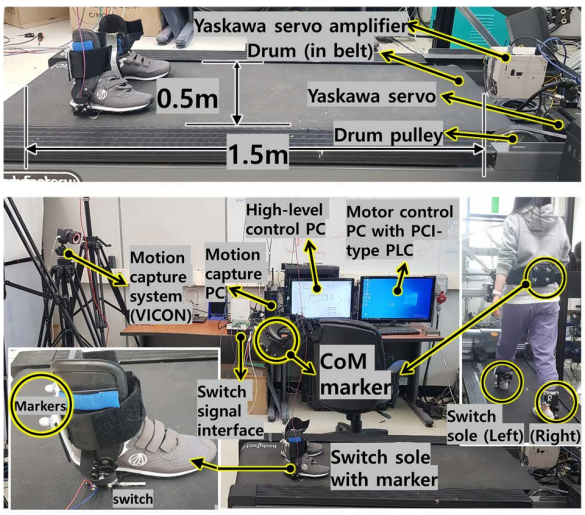

FIGURE 7. Experimental setup showing the PC used for executing the LI, marker locations, switch sole details, treadmill size and the used servomotor.

TABLE 1. Specifications of the UDT used in the experiment.

	Motor power	Drum pulley dia.	Servo pulley dia.	Drum dia.	Max. Belt speed
Spec.	1.8 kW	150*mm*	42*mm*	100*mm*	3.5*m/s*

the maximum belt speed of the developed UDT is 3.5 m/s. The user's pelvic and foot motions during treadmill walking were captured by the motion capture system (VICON) and used to measure x_1 and p_x with a sampling rate of 100 Hz. The markers for tracking the position of COM were placed on the posterior superior iliac spines. Considering the user's convenience and safety, these spinal markers were attached to the harness. The markers for tracking the ankles were attached to the switch soles that are specially designed soles installed in the user's ankle joint (see Figure 7). The switch soles have a movable joint so that they do not interfere with the movement of the user's ankle joint. The switches are active when the lower extremity that they are attached to is in the stance phase and deactivated during swing phase. During double support phase, p_x is computed as the average value of both the ankle positions, same as the simulation performed above.

If the user performs a run, the double support phase occurs in the air. Thus, the switch sole signals of both the lower extremities become temporarily off. At this time, since the position of the ankle joint of the lower extremity where the propulsive force is generated is located behind the ankle joint where the braking force and switch sole signals will be activated, p_x is decided to be the ankle joint having the smaller position value.

The hardware connection configuration is shown in Figure 8. The software running on each PC are executed in real-time with a 1kHz loop frequency, and real-time synchronization is realized by connecting the PCs through direct connected TCP/IP communication. The motion capture PC interfaces with the switch signals from the switch soles, and it measures the user's COM (x_1) and ankle joint position (p_x) via VICON. The measured information is transmitted to the high-level PC, and the control command (v_c) is generated. The low-level PC and the high-level PC transmit the current treadmill belt speed (v) and control command (v_c) to each other in real time. The PCI-type PLC installed in the low-level PC is connected to the servo amplifier via Mechatrolink, which is an open field network used to simplify system configuration while ensuring synchronization [27]. The loop frequency of the PLC used is guaranteed to be 10kHz, therefore, it can stably execute the calculated control command (v_c) given by the high-level control PC.

B. EXPERIMENTAL PROTOCOL

To obtain objective performance results, all the participants were given the same walking speed profile, and it was observed that how closely they were able to follow the given profile. The desired speed profile was provided visually to the participants through the graphic shown in Figure 9 (left),

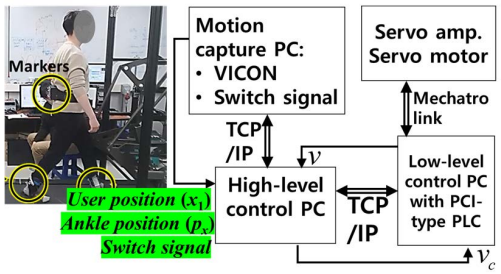

FIGURE 8. System configuration used for executing locomotion interface using the proposed IWS prediction method.

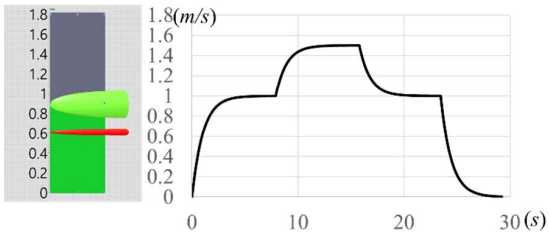

FIGURE 9. Visual display of the cue speed and current speed feedback (left), and the desired speed profile (right).

which was displayed on a monitor screen placed in front of them. The green indicator shows the cue speed consisted of the desired speed profile to a user, as shown in Figure 9 (right), while the red indicator shows the current treadmill speed (v), and the participants' task was to match the positions of both these indicators. To avoid excessive accelerations and to guarantee safety on the UDT, the acceleration and speed of the desired speed profile were limited to 1 m/s^2 and 1.5 m/s by applying a 1 second time constant to the step function. The profile indicating the cue speed starts at 0 m/s and then sequentially changed to 1 m/s, 1.5 m/s, 1 m/s and finally back to 0 m/s in 8 second intervals. Before the measured trials, the subjects practiced adjusting their walking according to the cue speeds 2-3 times. The same speed profile was tested under the two estimators (i.e., the research reported in [12] and the proposed method) in a randomized order.

For a fair comparison, the performance is considered to be equivalent if the same amount of position error exists when an arbitrary step input of the IWS is given to the existing and the proposed controller. The feedback controller used with both estimators had the same gain settings, while the gain of the linear observer was set to 6 through simulation. 10 young and healthy volunteers (5 men, 5 women) with ages ranging from 25 to 32 years (27.6 $\pm$ 7.0) and height 162-172 cm (167.2 $\pm$ 4.8), participated in this experiment. The experiments were conducted at room 202-1 of Dasan building, Gwangju Institute of Science and Technology (Gwangju, Republic of Korea), following the principles of the Declaration of Helsinki. The study protocol was approved by the Institutional Review Board of Gwangju Institute of Science and Technology (20210217-HR-59-06-04). Only the volunteers who had not experienced any musculoskeletal disease or injury in the past were included in the study. All participants provided written informed consent prior to inclusion in the study.

C. DATA ANALYSIS

From the collected data, the root mean square (RMS) of the error between the cue speed and the treadmill belt speed and RMS of error in user position are computed, respectively. Furthermore, to compare the gait pattern changes due to the existing and the proposed controllers, an analysis of the spatio-temporal gait parameters was performed on the treadmill, which included the total number of steps, average step length, cadence and walk ratio. The step length is measured when double stance is determined by the switch sole, which represents approximately the distance between the ipsilateral and the contralateral heel at each heel contact. The walk ratio represents the relationship between the amplitude and frequency of rhythmic leg movements during walking and was calculated as the average step length divided by the cadence [28]. Although cadence usually uses number of steps per minute, in this paper, it is defined as the number of steps per second since the experiment time was only 30s.

For post-experimental data analysis, a one-way repeated measures analysis of variance (RMANOVA) was performed to study the effects of the proposed controller under the various speed changes on the RMS of the error between the cue speed and the treadmill belt speed, RMS of the error in user position, total number of steps, average step length and walk ratio. Mauchly's test of Sphericity was used to confirm the validity of the RMANOVA results. Post hoc tests were conducted using the Bonferroni correction method. Partial eta squared (μ_p^2) was calculated as a measure of the effect size for one-way RMANOVA. All statistical analyses were carried out using SPSS V20.0 (IBM Corp., USA).

IV. RESULT

A. MAIN EXPERIMENTAL RESULTS

The average position error for all the participants, and its standard deviation (STD), in the time domain is shown in Figure 10. For synchronizing the results of each participant, post-processing was performed by referring to the cue speed data included in each participant's results. The yellow-shaded zone represents the accelerating and decelerating gait speeds. Both the controllers have relatively large position errors when the gait speed changes (yellow-shaded periods in Figure 10, except at the start and end of the experiment).

Figure 11 shows the time domain experimental results in the form of the average and STD of all the participants' walking speeds compared to the given cue speed profile. Analyzing both the LI controllers, the STD tends to increase at the beginning and end of the experiment. The reason for this large deviation in walking speeds of the participants at the beginning and ending periods is that they experience the incorrect speed convergence rate from the UDT, which is exacerbated by the large gait speed changes (1.5 m/s) during these periods as compared to the other experiment

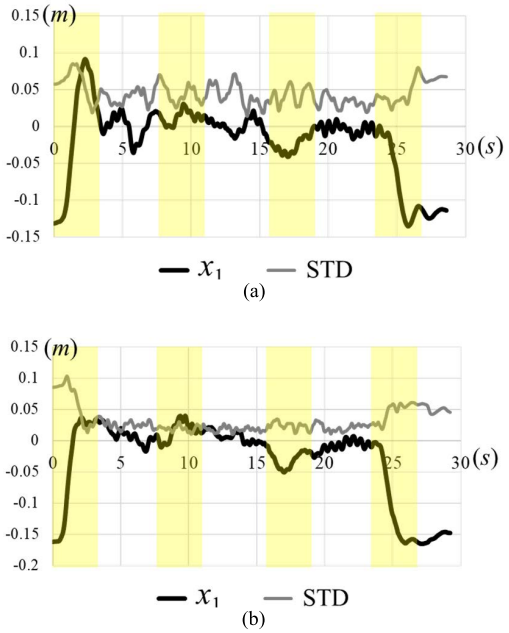

FIGURE 10. Time domain experimental results for the average of the position error and its standard deviation (STD), (a) existing controller and (b) proposed controller.

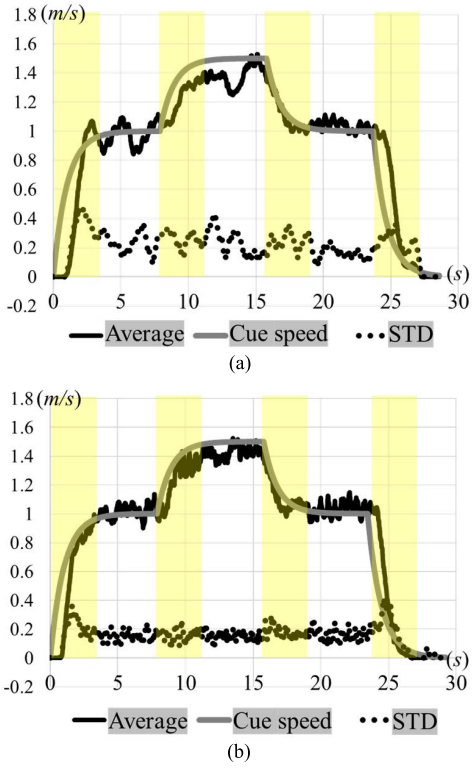

FIGURE 11. Time domain experimental results for the walking speed of all the participants compared to the desired velocity profile. (a) existing controller and (b) proposed controller.

periods [11]. This incorrect estimation of the gait speed transition makes it difficult for the subject to follow the desired speed cue, and as a result, an overshoot and undershoot are observed when the desired speed cue is considered as the reference input.

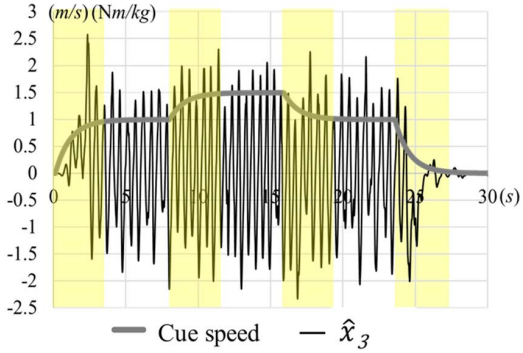

FIGURE 12. Estimated $\hat{x}_3$ of one subject representing T_{zmp}/m (Nm/kg).

However, when the user is trying to follow the desired speed cue with the existing method, there is a large difference in the gait speeds of the different participants. In the experiment period where the gait speed cue is maintained after accelerating or decelerating, the existing controller has more difficulty in following the cue speed. Thus, the trend of the STD remains larger than the proposed method.

Combining the experimental results for the cue speed following (command following) and the position error, the STD of the position error of each participant in Figure 10 and the gait speed error in Figure 11 show similar trends. That is, both the STDs of the existing controller show relatively larger errors and fluctuations. This is because the accuracy of gait speed estimation was reduced due to the generation of excessive control commands that did not match the intention of the participants who were trying to follow the speed cues. Thus, the current position robustness setting in the existing method is relatively unsuitable in this situation. It means that the IWS convergence rate should be lowered by a smaller gain in the linear observer, which will also reduce the position robustness. However, in the case of the presented IWS prediction, it can follow the IWS more precisely.

Figure 12 shows the estimated ankle torque per mass of a male participant with the speed cue. In the section at the start of the experiment, the ankle torque per mass ($\hat{x}_3$) showed a tendency to increase, reaching a maximum value of 2.7 Nm/kg. In the section where the walking speed is constant, the ankle torque shows a trend that is similar to the simulation results (1.5 Nm/kg) and the gait analysis research reported in [22] and [23]. When the cue for a reduction in walking speed is given, the ankle torque also tends to decrease, and reaches a minimum value of −2.3 Nm/kg. Thus, the proposed IWS estimator can predict the ankle joint torque well during the actual gait interface, similar to the simulation result presented in Figure 6(b).

B. STATISTICAL ANALYSIS OF THE MAIN RESULT

RMS of the error between the cue speed and the treadmill belt speed and RMS of the error in the user position for each participant is summarized in Table 2, and results of the one-way RMANOVA carried out to study the effects of the proposed controller are presented in Table 3. The average

TABLE 2. RMS results of each subject in the experiment.

Sub.	RMS of the error between the cue speed and the treadmill belt speed (m/s^2)		RMS of the error in the user position (m)	
	Existing	Proposed	Existing	Proposed
1	0.239147	0.190509	0.074423	0.071348
2	0.253012	0.20616	0.074858	0.076273
3	0.271649	0.215792	0.0811	0.101872
4	0.197322	0.175379	0.074941	0.085744
5	0.279051	0.245003	0.110542	0.090645
6	0.361598	0.204845	0.075015	0.100718
7	0.395726	0.188536	0.075101	0.045228
8	0.298328	0.212337	0.04913	0.069047
9	0.239393	0.241394	0.049318	0.064099
10	0.253107	0.214333	0.054523	0.048635

TABLE 3. Results of one-way RMANOVA of each set of RMS data.

Parameter	F	p-value	μ_p^2
RMS of the error between the cue speed and the treadmill belt speed	**(1, 9) =11.545**	**< 0.01**	**0.562**
RMS of error in user position	(1, 9) = .356	0.566	0.038

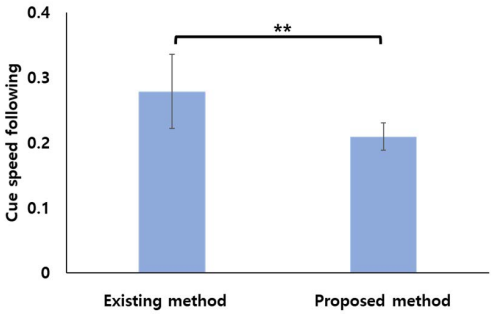

FIGURE 13. Mean and SD values of the RMS of the error between the cue speed and the treadmill belt speed. Statistically significant difference is marked based on Post-hoc pairwise comparison (**: p < 0.01).

values of the RMS of position error with the two different controllers are 0.072±0.017 m and 0.075±0.019 m, and there is no significant difference between them. The average values of the RMS of the error in following the cue speed were 0.279±0.057 m/s and 0.209±0.021 m/s, respectively, with the proposed controller showing significantly lower errors (p-value = 0.0028), as shown in Figure 13. The main reason for the increase in the cue speed following error, as compared to the existing controller, is that the walking speed of most of the participants fluctuated as they tried to follow the cue speed.

C. SPATIO-TEMPORAL GAIT PARAMETERS ANALYSIS

The total number of steps, average step length and walking ratio of all participants are summarized in Table 4, and results of the statistical analyses of these outcomes are presented in Table 5. The total number of steps with the existing controller (51.2±5.8 steps) was slightly but not significantly different from the proposed controller (49.8±4.89 steps). This means that the existing controller only slightly increases the cadence.

TABLE 4. Spatio-temporal gait parameters of all participants.

Sub.	Step number (No.)		Step length (m)		Walking ratio ($m/step/s$)	
	Existing	Propoesd	Existing	Propoesd	Existing	Propoesd
1	44	46	0.410	0.430	0.280	0.280
2	54	50	0.354	0.410	0.197	0.246
3	43	43	0.422	0.420	0.294	0.293
4	48	52	0.469	0.350	0.293	0.202
5	49	50	0.449	0.443	0.275	0.266
6	49	44	0.303	0.329	0.185	0.224
7	57	48	0.429	0.385	0.225	0.240
8	53	51	0.403	0.385	0.228	0.226
9	53	59	0.356	0.367	0.201	0.186
10	62	55	0.276	0.349	0.133	0.190

TABLE 5. Results of one-way RMANOVA of the gait parameter outcomes.

Parameter	F	p-value	μ_p^2
Step number	(1, 9) = 0.831	0.386	0.084
Step length	(1, 9) = 0.000	0.987	0.000
Walk ratio	(1, 9) = 0.001	0.754	0.011

In case of the step length, the existing and the proposed controller showed 0.3874±0.062 m and 0.3871±0.038 m, respectively. While for the walking ratio, the outcomes were 0.231±0.053 m/step/s and 0.235±0.036 m/step/s, respectively. There was also no significant difference in any of the spatio-temporal gait parameters. Thus, the overall results suggest that the proposed controller has relatively better performance in following the IWS and it does not change the user's gait pattern. Moreover, after the experiment, we asked each participant about their feelings or opinions about both the controllers. All the participants were of the opinion that it was easier to follow the speed cues with the LI controller that utilized the proposed IWS prediction method. This perception is supported by the result obtained from the quantitative data.

V. CONCLUSION

In this paper, we proposed an IWS estimator that uses the position information of the ankle joint and the COM of the subject, which is more accurate and sensitive than the conventional method. The acceleration/deceleration generated during walking is set as the disturbance of the UDT system, and the torque generated at the ankle joint, which is the cause of this disturbance, is accurately predicted by the proposed observer scheme to quickly respond to the IWA by using the 1st and 2nd order dynamics that represent the UDT-human dynamics. Results from the experiments with 10 participants show that, as compared to the previously developed method, the proposed controller has significantly better performance in following the user's IWS, while maintaining the same level of position robustness and having no significant effect on their gait pattern.

REFERENCES

[1] B. Hejrati, K. L. Crandall, J. M. Hollerbach, and J. J. Abbott, "Kinesthetic force feedback and belt control for the treadport locomotion interface," *IEEE Trans. Haptics*, vol. 8, no. 2, pp. 176–187, Apr./Jun. 2015.

[2] K. K. Patel and S. K. Vij, "Locomotion interface to the virtual environment to acquire spatial knowledge," Presented at the TENCON, Hyderabad, India, Nov. 2008.
[3] B. J. Mohler, W. B. Thompson, S. H. Creem-Regehr, P. Willemsen, H. L. Pick, Jr., and J. J. Rieser, "Calibration of locomotion resulting from visual motion in a treadmill-based virtual environment," *ACM Trans. Appl. Perception*, vol. 4, no. 1, p. 4, Jan. 2007.
[4] F. Alton, L. Baldey, S. Caplan, and M. C. Morrissey, "A kinematic comparison of overground and treadmill walking," *Clin. Biomech.*, vol. 13, no. 6, pp. 434–440, Sep. 1998.
[5] J. Yoon, H.-S. Park, and D. L. Damiano, "A novel walking speed estimation scheme and its application to treadmill control for gait rehabilitation," *J. NeuroEng. Rehabil.*, vol. 9, no. 1, pp. 1–13, Dec. 2012.
[6] J. Kim, C. J. Stanley, L. A. Curatalo, and H.-S. Park, "A user-driven treadmill control scheme for simulating overground locomotion," in *Proc. Annu. Int. Conf. IEEE Eng. Med. Biol. Soc.*, Aug. 2012, pp. 3061–3064.
[7] A. De Luca, R. Mattone, and P. R. Giordano, "Acceleration-level control of the CyberCarpet," in *Proc. IEEE Int. Conf. Robot. Autom.*, Apr. 2007, pp. 2330–2335.
[8] E. Panteley and A. Loría, "On global uniform asymptotic stability of nonlinear time-varying systems in cascade," *Syst. Control Lett.*, vol. 33, no. 2, pp. 131–138, 1998.
[9] H. J. Asl, S.-H. Pyo, and J. Yoon, "An intelligent control scheme to facilitate abrupt stopping on self-adjustable treadmills," in *Proc. IEEE Int. Conf. Robot. Autom. (ICRA)*, May 2018, pp. 1639–1644.
[10] A. E. Minetti, L. Boldrini, L. Brusamolin, P. Zamparo, and T. McKee, "A feedback-controlled treadmill (treadmill-on-demand) and the spontaneous speed of walking and running in humans," *J. Appl. Physiol.*, vol. 95, no. 2, pp. 838–843, Aug. 2003.
[11] L. Litchtenstein, J. Barabas, R. L. Woods, and E. Peli, "A feedback control instrument for treadmill locomotion in virtual environments," *ACM Trans. Appl. Perception*, vol. 4, no. 1, pp. 1–17, 2007.
[12] J. L. Souman, P. R. Giordano, M. Schwaiger, I. Frissen, T. Thümmel, H. Ulbrich, A. D. Luca, H. H. Bülthoff, and M. O. Ernst, "CyberWalk: Enabling unconstrained omnidirectional walking through virtual environments," *ACM Trans. Appl. Perception*, vol. 8, no. 4, pp. 25–46, 2011.
[13] J. Kim, H.-S. Park, and D. L. Damiano, "An interactive treadmill under a novel control scheme for simulating overground walking by reducing anomalous force," *IEEE/ASME Trans. Mechatronics*, vol. 20, no. 3, pp. 1491–1496, Jun. 2015.
[14] S. Kajita, F. Kanehiro, K. Kaneko, K. Fujiwara, K. Harada, K. Yokoi, and H. Hirukawa, "Biped walking pattern generation by using preview control of zero-moment point," in *Proc. IEEE Int. Conf. Robot. Autom.*, Sep. 2003, pp. 1620–1626.
[15] Y. Choi, D. Kim, Y. Oh, and B. J. You, "Posture/walking control for humanoid robot based on kinematic resolution of CoM Jacobian with embedded motion," *IEEE Trans. Robot.*, vol. 23, no. 6, pp. 1285–1293, Dec. 2007.
[16] N. Fischer, D. Hughes, P. Walters, E. M. Schwartz, and W. E. Dixon, "Nonlinear RISE-based control of an autonomous underwater vehicle," *IEEE Trans. Robot.*, vol. 30, no. 4, pp. 845–852, Aug. 2014.
[17] Z. Yang, J. Ji, X. Sun, H. Zhu, and Q. Zhao, "Active disturbance rejection control for bearingless induction motor based on hyperbolic tangent tracking differentiator," *IEEE J. Emerg. Sel. Topics Power Electron.*, vol. 8, no. 3, pp. 2623–2633, Sep. 2020.
[18] B. R. Bloem, J. M. Hausdorff, J. E. Visser, and N. Giladi, "Falls and freezing of gait in Parkinson's disease: A review of two interconnected, episodic phenomena," *Movement Disorders, Off. J. Movement Disorder Soc.*, vol. 19, no. 8, pp. 871–884, Aug. 2004.
[19] B.-Z. Guo and Z.-L. Zhao, "On convergence of tracking differentiator," *Int. J. Control*, vol. 84, no. 4, pp. 693–701, Apr. 2011.
[20] W. Liu, S. Y. Chen, and H. X. Huang, "Second-order hierarchical fast terminal sliding model control for a class of underactuated systems using disturbance observer," *Automat., Control Intell. Syst.*, vol. 7, no. 2, pp. 65–78, 2019.
[21] X. Yang and Y. Huang, "Capabilities of extended state observer for estimating uncertainties," in *Proc. IEEE Amer. Control Conf.*, Jun. 2009, pp. 3700–3705.
[22] P.-C. Kao, C. L. Lewis, and D. P. Ferris, "Joint kinetic response during unexpectedly reduced plantar flexor torque provided by a robotic ankle exoskeleton during walking," *J. Biomech.*, vol. 43, no. 7, pp. 1401–1407, May 2010.
[23] C. F. Ong, T. Geijtenbeek, J. L. Hicks, and S. L. Delp, "Predicting gait adaptations due to ankle plantarflexor muscle weakness and contracture using physics-based musculoskeletal simulations," *PLOS Comput. Biol.*, vol. 15, no. 10, Oct. 2019, Art. no. e1006993.
[24] Y. X. Su, C. H. Zheng, D. Sun, and B. Y. Duan, "A simple nonlinear velocity estimator for high-performance motion control," *IEEE Trans. Ind. Electron.*, vol. 52, no. 4, pp. 1161–1169, Aug. 2005.
[25] M. Haijie, L. Wei, and X. Feng, "Nonlinear tracking differentiator design based on hyperbolic tangent," *Comput. Appl.*, vol. 36, no. 1, pp. 305–309, 2016.
[26] B. Xian, D. M. Dawson, M. S. D. Queiroz, and J. Chen, "A continuous asymptotic tracking control strategy for uncertain nonlinear systems," *IEEE Trans. Autom. Control*, vol. 49, no. 7, pp. 1206–1211, Jul. 2004.
[27] *An Overview of MECHATROLINK-III*. Accessed: Jun. 7, 2021. [Online]. Available: http://www.mechatrolink.org/en/mechatrolink/feature-m3.html
[28] Y. P. Lim, Y.-C. Lin, and M. G. Pandy, "Effects of step length and step frequency on lower-limb muscle function in human gait," *J. Biomech.*, vol. 57, pp. 1–7, May 2017.

SANGHUN PYO received the B.E. and M.S. degrees from the School of Mechanical Engineering, Gyeongsang National University, Jinju, South Korea, in 2012 and 2014, respectively. He is currently pursuing the Ph.D. degree with the Gwangju Institute of Science and Technology (GIST), Gwangju, South Korea. From 2016 to 2017, he was a Ph.D. Researcher with GIST. In 2018, he joined the School of Integrated Technology, GIST. He was a Teaching Assistance in mechatronics, control, and robot kinematics with GIST, from 2018 to 2020. He is also researching at the Intelligent Medical Robotics Laboratory and the Cognition and Intelligence Laboratory, GIST. His current research interests include robotics, control theory, locomotion interface, and omnidirectional treadmill (ODT).

HOSU LEE received the B.E. and M.S. degrees from the School of Mechanical Engineering, Gyeongsang National University, Jinju, South Korea, in 2014 and 2016, respectively, the Ph.D. degree from Gyeongsang National University, in 2017, and the Ph.D. degree from the Department of Mechatronics, Gwangju Institute of Science and Technology (GIST), Gwangju, South Korea, in 2022. From 2016 to 2017, he joined as a Researcher with Gyeongsang National University. He worked as a Teaching Assistance in mechatronics, robotics at GIST, from 2019 to 2021. He is currently working as a Postdoctoral Researcher at the Intelligent Medical Robotics Laboratory and the Cognition and Intelligence Laboratory, GIST. His current research interests include rehabilitation robotics, haptic feedback interfaces, cable driven parallel robot (CDPR), and locomotion interface.

JUNGWON YOON (Member, IEEE) received the Ph.D. degree from the Department of Mechatronics, Gwangju Institute of Science and Technology (GIST), Gwangju, South Korea, in 2005. From 2005 to 2017, he was a Professor with the School of Mechanical and Aerospace Engineering, Gyeongsang National University, Jinju, South Korea. In 2017, he joined the School of Integrated Technology, GIST, where he is currently a Professor. He has authored or coauthored more than 80 peer-reviewed journal articles and patents. His current research interests include bio-nano robot control, virtual reality haptic devices, and rehabilitation robots. He was a Technical Editor of the IEEE/ASME TRANSACTIONS ON MECHATRONICS and an Associate Editor of *Frontiers in Robotics and AI*.